Inorg. Chem. **2005**, *44*, 9335–9339

Synthesis, Crystal Structure, and Solid-State NMR Spectroscopy of a Salt-Inclusion Stannosilicate: $[Na_3F][SnSi_3O_9]$

Chen-Hui Liao,[†] Pai-Ching Chang,[†] Hsien-Ming Kao,*[,†] and Kwang-Hwa Lii*[,†,‡]

Department of Chemistry, National Central University, Chungli, Taiwan, Republic of China, and Institute of Chemistry, Academia Sinica, Taipei, Taiwan, Republic of China

Received August 18, 2005

A salt-inclusion stannosilicate, $[Na_3F][SnSi_3O_9]$, has been synthesized using a flux-growth method and characterized by single-crystal X-ray diffraction. The structure consists of six-membered silicate rings linked via corner sharing by $Sn^{IV}O_6$ octahedra to form a 3-D framework that delimits two types of channels. The F atoms and Na atoms are located in the structural channels and form a dimer with the anti-Al_2Cl_6(g) structure. This stannosilicate adopts a new structure and is the first metal silicate that contains both Na^+ and F^- ions in the channels. The ^{19}F and ^{29}Si MAS NMR and ^{23}Na MQMAS NMR spectra are consistent with the crystallographic results.

Introduction

Recently, a good number of salt-inclusion phosphates, arsenates, and silicates have been synthesized mainly by employing molten-salt methods at high temperatures.[1−6] Several metal oxalates containing alkali halides have also been synthesized by a hydrothermal method at ca. 150 °C.[7−9] These salt-inclusion compounds contain some extraordinary structural features. For example, the structure of $K_2Cs_3Cu_3(P_2O_7)_2Cl_3$ consists of 8- and 16-ring channels, in which CsCl and KCl/CsCl salt reside, respectively. The salt can be removed by washing at room temperature to give a microporous compound.[1] In some of these mixed ionic and covalent solids, the incorporated salt sublattices are made of chlorine-centered acentric secondary building units, thus forming noncentrosymmetric phosphate and silicate frameworks.[4−6] The metathetic reaction between $CdCl_2$ and $K_2C_2O_4$ under hydrothermal conditions yields $[KCl][Cd_6(C_2O_4)_6]\cdot 2H_2O$, containing Cd_6O_{24} clusters with the Cl^- anions in the center. The KCl sublattice forms an ordered 3-D rock-salt structure with a unit cell length double that of the normal state phase.[7] A series of chromous disilicates ($Cr_3Si_2O_7\cdot {}^1/_4MX$, MX = NaCl, NaBr, KCl, KBr) hosting alkali-metal halides in a framework structure were reported.[10] The alkali-metal cations and halide anions are located in different cages in the structure.

We have been interested in the exploratory synthesis of mixed octahedral−tetrahedral framework oxides and have synthesized a number of new silicates of transition metals,[11a,b] main-group elements,[11c−f] and uranium[11g−i] by high-temperature, high-pressure hydrothermal reactions in gold ampules at 500−600 °C. In an attempt to extend our studies to explore whether we can synthesize new metal silicates by using a flux-growth method, we obtained a salt-inclusion compound, $[Na_3F][SnSi_3O_9]$ (denoted as **1**). This new compound is the first metal silicate that contains both Na^+ and F^- ions in the structural channels. In this paper, we describe the molten-salt synthesis, crystal structure, and solid-state NMR spec-

* To whom correspondence should be addressed. E-mail: liikh@cc.ncu.edu.tw (K.-H.L), hmkao@cc.ncu.edu.tw (H.-M.K).
† National Central University.
‡ Academia Sinica.

(1) Huang, Q.; Ulutagay, M.; Michener, P. A.; Hwu, S.-J. *J. Am. Chem. Soc.* **1999**, *121*, 10323.
(2) Huang, Q.; Hwu, S.-J.; Mo, X. *Angew. Chem., Int. Ed.* **2001**, *40*, 1690.
(3) Hwu, S.-J.; Ulutagay-Kartin, M.; Clayhold, J. A.; Mackay, R.; Wardojo, T. A.; O'Connor, C. J.; Krawiec, M. *J. Am. Chem. Soc.* **2002**, *124*, 12404.
(4) Huang, Q.; Hwu, S.-J. *Inorg. Chem.* **2003**, *42*, 655.
(5) Mo, X.; Hwu, S.-J. *Inorg. Chem.* **2003**, *42*, 3978.
(6) Mo, X.; Ferguson, E.; Hwu, S.-J. *Inorg. Chem.* **2005**, *44*, 3121.
(7) Vaidhyanathan, R.; Neeraj, S.; Prasad, P. A.; Natarajan, S.; Rao, C. N. R. *Angew. Chem., Int. Ed.* **2000**, *39*, 3470.
(8) Vaidhyanathan, R.; Natarajan, S.; Rao, C. N. R. *J. Solid State Chem.* **2002**, *167*, 274.
(9) Vaidhyanathan, R.; Natarajan, S.; Rao, C. N. R. *Mater. Res. Bull.* **2003**, *38*, 477.
(10) Schmidt, A.; Glaum, R. *Inorg. Chem.* **1997**, *36*, 4883.
(11) (a) Li, C.-Y.; Hsieh, C.-Y.; Lin, H.-M.; Kao, H.-M.; Lii, K.-H. *Inorg. Chem.* **2002**, *41*, 4206. (b) Kao, H.-M.; Lii, K.-H. *Inorg. Chem.* **2002**, *41*, 5644. (c) Hung, L.-I.; Wang, S.-L.; Kao, H.-M.; Lii, K.-H. *Inorg. Chem.* **2003**, *42*, 4057. (d) Huang, L.-I.; Wang, S.-L.; Szu, S.-P.; Hsieh, C.-Y.; Kao, H.-M.; Lii, K.-H. *Chem. Mater.* **2004**, *16*, 1660. (e) Huang, L.-I.; Wang, S.-L.; Chen, C.-Y.; Chang, B.-C.; Lii, K.-H. *Inorg. Chem.* **2005**, *44*, 2992. (f) Lo, F.-R.; Lii, K.-H. *J. Solid State Chem.* **2005**, *178*, 1017. (g) Chen, C.-S.; Kao, H.-M.; Lii, K.-H. *Inorg. Chem.* **2005**, *44*, 935. (h) Chen, C.-S.; Chiang, R. K.; Kao, H.-M.; Lii, K.-H. *Inorg. Chem.* **2005**, *44*, 3914. (i) Chen, C.-S.; Lee, S.-F.; Lii, K.-H. *J. Am. Chem. Soc.* **2005**, *127*, 12208.

10.1021/ic0514086 CCC: $30.25
Published on Web 10/21/2005

troscopy of this interesting salt-inclusion stannosilicate. In particular, the ^{23}Na multiple quantum magic angle spinning (MQMAS) method has been applied to obtain high-resolution NMR spectra and quadrupolar parameters of distinct Na sites.[12]

Experimental Section

Synthesis. A mixture of 0.5 g of NaF (Merck, >99%), 0.5 g of V_2O_5 (Merck, >99%), 0.1202 g of SiO_2 (Cerac, 99.99%), and 0.0753 g of SnO_2 (Aldrich, 99.9%) (Na/Si/Sn mole ratio of 23.8:4:1) was placed in a 4-mL platinum crucible, heated to 700 °C, and isothermed for 10 h, followed by slow cooling to 500 °C at 2 °C/h and then furnace cooling to room temperature. The flux was dissolved with hot water, and the solid product was obtained by suction filtration. The reaction produced 0.0905 g of colorless plate crystals. A qualitative energy-dispersive X-ray analysis of several colorless crystals confirmed the presence of Na, Sn, and Si. The bulk product was monophasic, as indicated by powder X-ray diffraction (Figure S1 in the Supporting Information). Compound **1** was the only nonsoluble phase in hot water, and the yield was 41.6%. The sample was used for solid-state NMR study.

Single-Crystal X-ray Diffraction. A suitable crystal of **1** with dimensions 0.05 × 0.05 × 0.03 mm^3 was selected for indexing and intensity data collection on a Siemens SMART CCD diffractometer equipped with a normal focus, 3-kW sealed-tube X-ray source. Intensity data were collected at room temperature in 1271 frames with ω scans (width of 0.30° per frame). The number of observed unique reflections [$F_o > 4\sigma(F_o)$] is 1115 ($2\theta_{max} = 56.54°$; $R_{int} = 0.0206$). The program SADABS was used for the absorption correction ($T_{min}/T_{max} = 0.933/0.985$).[13] The structure was solved by direct methods and difference Fourier syntheses. The Na and F atoms sites in the structural tunnels are ordered and fully occupied. The final cycles of least-squares refinement included atomic coordinates and anisotropic thermal parameters for all atoms (number of parameters = 83). The final difference Fourier maps were flat ($\Delta\rho_{max,min} = 0.45, -0.65$ e/Å^3). All calculations were performed using the SHELXTL version 5.1 software package.[14]

Solid-State NMR Measurements. ^{19}F, ^{29}Si, and ^{23}Na MAS NMR spectra at 293 K were acquired on a Varian Infinityplus-500 NMR spectrometer equipped with a 4-mm Chemagnetics T3 HFX probe. The 1-D ^{23}Na MAS NMR spectra were obtained with a small flip angle of approximately 15° (0.6 μs) and with a cycle delay of 2 s. ^{19}F MAS NMR spectra were acquired with a 90° pulse of 4.5 μs and a recycle delay of 15 s. A 45° pulse of 3.0 μs and a recycle delay of 50 s were used to acquire the ^{29}Si NMR spectra. The spinning speed was set to 16 kHz for ^{19}F and ^{23}Na NMR. ^{19}F, ^{29}Si, and ^{23}Na NMR chemical shifts were externally referenced to $CFCl_3$, tetramethylsilane (TMS), and a 1 M aqueous NaCl solution at 0 ppm, respectively.

^{23}Na MQMAS NMR spectra were obtained using a three-pulse sequence with *z* filtering.[15] The length of the first and second hard pulses ($B_1 = 110$ kHz) used to excite the triple-quantum coherences (±3Q) and to transfer them back to zero quantum were 6.50 and 1.75 μs, respectively. A soft pulse of 11.50 μs ($B_1 = 22$ kHz) was applied after the *z*-filter period (200 μs). To produce pure absorption-mode line shapes in 2-D spectra, the hypercomplex method was applied for data collection.[16] Typically, 128 data points (312 transients for each point) were acquired in the t_1 dimension in increments of 31 μs. The MQMAS data were processed with a shearing transformation prior to Fourier transformation with respect to t_1 to obtain a 2-D spectrum with an isotropic frequency component along the F_1 spectral axis and an anisotropic frequency along the F_2 axis. The F_2 slices corresponding to each Na site were then extracted and simulated with the STARS software in order to estimate the quadrupolar parameters.[17]

Table 1. Crystallographic Data for $[Na_3F][SnSi_3O_9]$

chemical formula	$FO_9Na_3Si_3Sn$
a/Å	10.539(1)
b/Å	13.953(2)
c/Å	6.5171(7)
β/deg	111.576(2)
V/Å^3	891.2(3)
Z	4
formula weight	434.93
space group	*C*2/*m* (No. 12)
T, °C	23
λ(Mo Kα), Å	0.71073
D_{calc}, g/cm^3	3.241
μ(Mo Kα), cm^{-1}	34.7
R1[a]	0.0161
wR2[b]	0.0422

[a] $R1 = \sum||F_o| - |F_c||/\sum|F_o|$. [b] $wR2 = [\sum w(F_o^2 - F_c^2)^2/\sum w(F_o^2)^2]^{1/2}$, $w = 1/[\sigma^2(F_o^2) + (aP)^2 + bP]$, $P = [\max(F_o^2,0) + 2(F_c)^2]/3$, where $a = 0.02$ and $b = 0.89$.

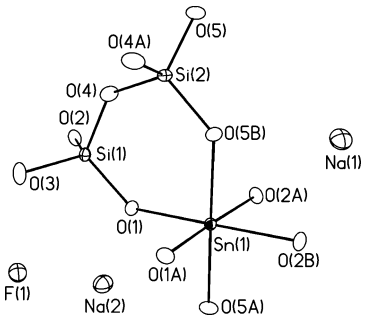

Figure 1. Building units of **1** showing the atom labeling scheme. Thermal ellipsoids are shown at 50% probability.

Table 2. Selected Bond Lengths (Å) for $[Na_3F][SnSi_3O_9]$

Sn(1)−O(1)	2.032(1) (2×)	Sn(1)−O(2)	2.036(2) (2×)
Sn(1)−O(5)	2.057(2) (2×)	Si(1)−O(1)	1.609(2)
Si(1)−O(2)	1.611(2)	Si(1)−O(3)	1.6181(9)
Si(1)−O(4)	1.645(2)	Si(2)−O(4)	1.631(2) (2×)
Si(2)−O(5)	1.606(2)	(2×)Na(1)−F(1)	2.193(2)
Na(1)−F(1)	2.259(3)	Na(1)−O(2)	2.413(2) (2×)
Na(1)−O(2)	2.836(2)	(2×)Na(2)−F(1)	2.113(1)
Na(2)−O(1)	2.301(2)	Na(2)−O(4)	2.325(2)
Na(2)−O(5)	2.408(2)	Na(2)−O(5)	2.860(2)

Results and Discussion

Structure. The crystallographic data are given in Table 1 and selected bond lengths and bond angles in Table 2. As shown in Figure 1, the structure of **1** is constructed from the following structural elements: 2 SiO_4 tetrahedra, 1 SnO_6 octahedron, and 1 F and 2 Na atoms. Na(1), F(1), and O(3)

(12) Frydman, L.; Harwood, J. S. *J. Am. Chem. Soc.* **1995**, *117*, 5367.
(13) Sheldrick, G. M. *SADABS, Program for Siemens Area Detector Absorption Corrections*; University of Göttingen, Göttingen, Germany, 1997.
(14) Sheldrick, G. M. *SHELXTL Programs*, version 5.1; Bruker AXS GmbH: Karlsruhe, Germany, 1998.
(15) Amoureux, J. P.; Fernandez, C.; Steuernagel, S. *J. Magn. Reson., Ser. A* **1996**, *123*, 116.
(16) States, D. J.; Haberkorn, R. A.; Ruben, D. J. *J. Magn. Reson.* **1982**, *48*, 286.
(17) Jakobsen, H. J.; Skibstedt, J.; Bildsoe, H.; Nielsen, N. C. *J. Magn. Reson.* **1989**, *85*, 173.

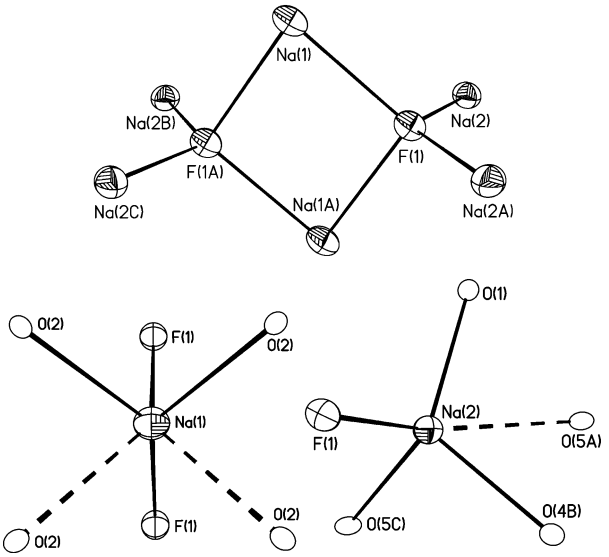

Figure 2. Coordination environments of Na and F atoms in **1**. The dashed lines represent the longer Na−O bonds.

lie in mirror planes, SnO_6 and $Si(2)O_4$ have a local symmetry of C_2, and all other atoms are at general positions. The observed Si−O bond lengths (1.606−1.645 Å, average 1.620 Å) and O−Si−O bond angles (106.3−114.0°) are typical values and are within the normal range.[18] Each SiO_4 is bonded to two SiO_4 tetrahedra and two SnO_6 octahedra. All O atoms except O(3) coordinate to Na atoms. The SnO_6 octahedron is quite regular, with the Sn−O bond lengths in the range from 2.032 to 2.057 Å. The bond-valence sum for Sn(1) is 4.15, indicating that the Sn atom is tetravalent.[19] Each SnO_6 octahedron shares its corners with six different SiO_4 tetrahedra. All Na and F sites are fully occupied. The coordination environments of Na and F atoms are shown in Figure 2. Na(1) is bonded to 2 F and 4 O atoms with CN (coordination number) = 4 + 2, with the first number referring to the number of neighboring atoms at shorter distances, and Na(2) is bonded to 1 F and 4 O atoms with CN = 4 + 1. The Na atoms and four-coordinate F atoms form a dimer with the anti-Al_2Cl_6(g) structure. It should be noted that the Na atoms are also bonded to framework O atoms.

The structure of **1** consists of six-membered single rings of corner-sharing SiO_4 tetrahedra in the (20−1) plane linked together via corner sharing by a single SnO_6 octahedron to form a 3-D framework that delimits two types of channels (Figure 3). The first type is along the *a* axis and is formed by stacking the six-membered silicate rings, and the second type is along the *b* and *c* axes and is formed by the edges of 2 SnO_6 octahedra and 4 SiO_4 tetrahedra. The minimum O···O distance across the six-membered silicate ring less one O diameter of 2.76 Å is 2.10 Å, which is slightly greater than the diameter for a six-coordinate Na^+ ion (2.04 Å). Therefore, the window should be large enough for the Na^+ ion to pass through. In contrast, the second type of window is too narrow to allow the Na^+ ion to squeeze through at

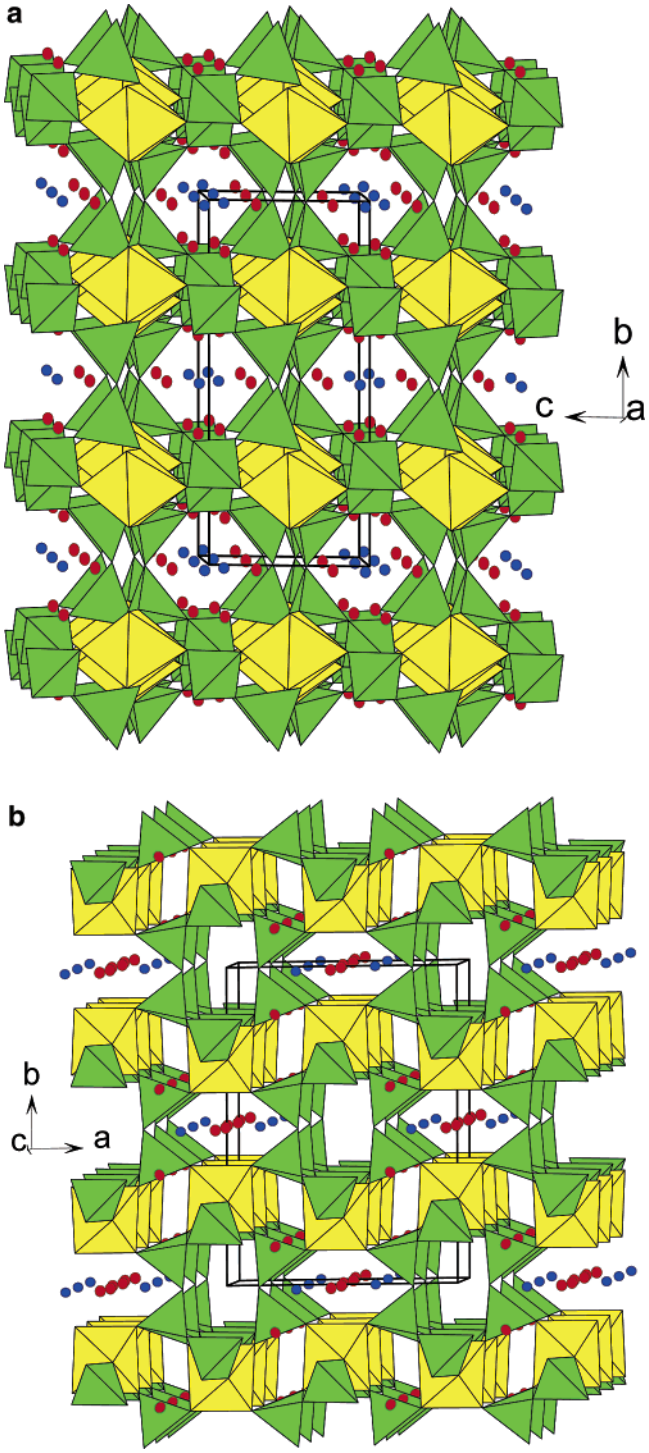

Figure 3. (a) Structure of **1** viewed along the *a* axis. The yellow and green polyhedra represent SnO_6 octahedra and SiO_4 tetrahedra, respectively. Red circles: Na atoms. Blue circles: F atoms. (b) Structure of **1** viewed along the *c* axis.

room temperature. Although the channels along the *a* axis are open enough for ion passage, the Na^+ ions are tightly bound with F^- ions and the framework O atoms, as indicated by approximately isotropic thermal vibrations and the valence sums of 0.96 and 1.06 for Na(1) and Na(2), respectively. The F_2Na_6 unit is located in a cage surrounded by 10 six-membered rings and several smaller rings (Figure 4).

Several stannosilicates with the general formula $A_2SnSi_3O_9 \cdot nH_2O$ have been reported. $K_2SnSi_3O_9 \cdot H_2O$ (named

(18) Liebau, F. *Structural Chemistry of Silicates: Structure, Bonding and Classification*; Springer-Verlag: Berlin, 1985.
(19) Brown, I. D.; Altermatt, D. *Acta Crystallogr.* **1985**, *B41*, 244.

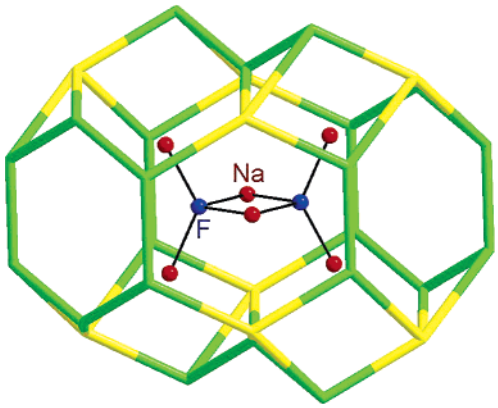

Figure 4. F_2Na_6 unit in a cage in the structure of **1**. In this simplified schematic diagram, the tetrahedral Si and octahedral Sn atoms are located at the intersections of the lines, as O bridges are made by corner sharing from the vertexes of the tetrahedron and octahedron.

AV-6)[20] adopts the structure of the rare mineral umbite ($K_2ZrSi_3O_9 \cdot H_2O$).[21] $K_2SnSi_3O_9$ (AV-11) was synthesized by calcining AV-6 in air at high temperature.[22] Both AV-6 and AV-11 contain infinite chains of corner-sharing SiO_4 tetrahedra. However, in the structure of AV-6, the infinite chain has a period of three tetrahedra, while in the structure of AV-11, the chain has a period of six tetrahedra. The sodium stannosilicate $Na_2SnSi_3O_9 \cdot 2H_2O$ (AV-10) has a new structure.[23] Although both AV-10 and AV-11 contain infinite silicate chains with a period of six tetrahedra, the chains are connected by SnO_6 octahedra in different ways. A sodium chloride stannosilicate, $Na_{2.26}SnSi_3O_9Cl_{0.26} \cdot xH_2O$ (AV-13), was reported, and its 3-D framework structure consists of six-membered $[Si_6O_{18}]^{12-}$ rings, which are interconnected by SnO_6 octahedra.[24] Each Na^+ cation in the structural channel is five-coordinated to three framework O atoms, one water molecule, and a fifth ligand, which may be a second water molecule or a chloride anion. All of the stannosilicates in the AV-*n* family were synthesized under hydrothermal conditions in a Teflon-lined autoclave at 200−230 °C and structurally characterized by powder X-ray diffraction. Recently, we reported a cesium stannosilicate, $Cs_2SnSi_3O_9$, which was synthesized by a high-temperature, high-pressure hydrothermal method and characterized by single-crystal X-ray diffraction.[11f] Its structure is closely related to that of AV-10. Compound **1** adopts a new structure and is the first salt-inclusion metal silicate that contains F^- ions in the structural channels. This interesting compound also suggests the utility of salt inclusion in the synthesis of new framework silicates.

MAS NMR. The ^{19}F MAS NMR spectrum of **1** (Figure 5a) shows a sharp resonance at −219 ppm, which corresponds to the single F(4Na) environment in the structure. For comparison, the ^{19}F MAS NMR spectrum of solid NaF shows a single peak at −221 ppm. Two resonances at −88 and −94 ppm with an intensity ratio of 1:2 are observed in the ^{29}Si MAS NMR spectrum of **1** (Figure 5b). It has been recognized that the ^{29}Si NMR chemical shift depends on the average value of the four Si−O−T bond angles and shifts upfield with increasing Si−O−T bond angle.[25] The average bond angles are 137.6° and 134.9° for Si(1) and Si(2), respectively. The peak at −94 ppm is therefore assigned to

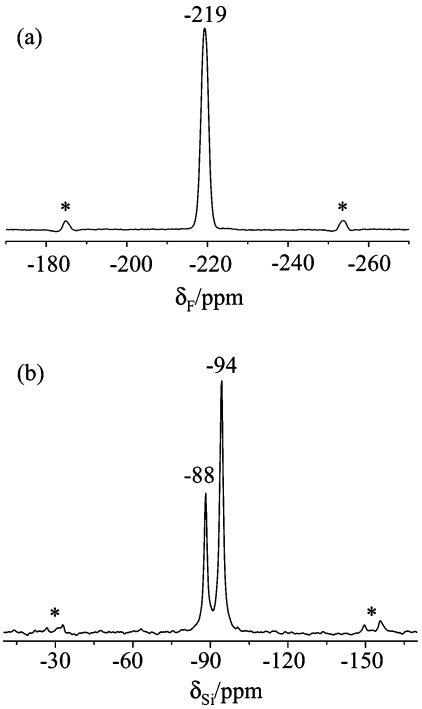

Figure 5. (a) ^{19}F and (b) ^{29}Si MAS NMR spectra of **1**, acquired at spinning speeds of 16 and 6 kHz, respectively. Asterisks denote spinning sidebands.

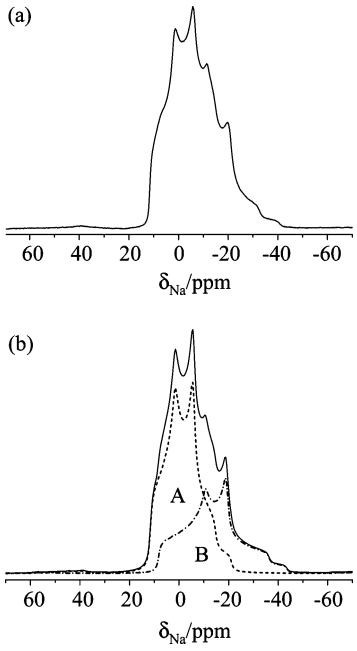

Figure 6. (a) Experimental and (b) simulated 1-D ^{23}Na MAS NMR spectra of **1**. The simulated total spectrum in (b, solid line) is the sum of A and B subspectra (dashed lines) with a 2:1 intensity ratio. The NMR parameters used for producing A and B subspectra are as follows: $\delta_{iso}(A) = 12.5$ ppm, $C_Q(A) = 3.0$ MHz, $\eta_Q(A) = 0.55$; $\delta_{iso}(B) = 9.0$ ppm, $C_Q(B) = 3.7$ MHz, $\eta_Q(B) = 0.68$.

(20) Lin, Z.; Rocha, J.; Valente, A. *Chem. Commun.* **1999**, *24*, 2489.
(21) Poojary, D. M.; Bortun, A. I.; Bortun, L. N.; Clearfield, A. *Inorg. Chem.* **1997**, *36*, 3072.
(22) Lin, Z.; Ferreira, A.; Rocha, J. *J. Solid State Chem.* **2003**, *175*, 258.
(23) Ferreira, A.; Lin, Z.; Rocha, J.; Morais, C. M.; Lopes, M.; Fernandez, C. *Inorg. Chem.* **2001**, *40*, 3330.
(24) Ferreira, A.; Lin, Z.; Soares, M. R.; Rocha, J. *Inorg. Chim. Acta* **2003**, *356*, 19.

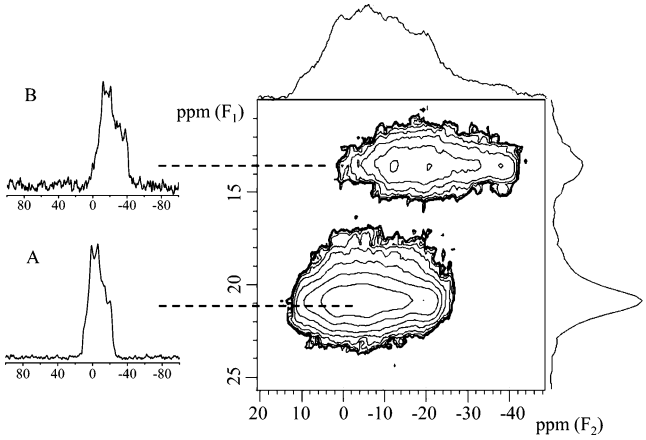

Figure 7. 2-D ^{23}Na MQMAS spectrum of **1**, together with F_1 and F_2 projections, and F_2 slices corresponding to the two crystallographically inequivalent Na sites.

Si(1) and the other peak (−88 ppm) to Si(2). The peak intensities are also consistent with the assignment. The 1-D ^{23}Na MAS NMR spectrum of **1** (Figure 6a), on the other hand, exhibits broad and complex line shapes characteristic of second-order quadrupolar interactions of the ^{23}Na nucleus ($I = {}^3/_2$). There are two distinct Na sites, as determined by X-ray diffraction. Therefore, the broad and complex line shapes consist of two overlapping signals, which hinder us from deriving the quadrupolar parameters of the Na atoms.

^{23}Na MQMAS NMR experiments were performed in order to resolve the complex spectrum. As shown in Figure 7, the result reveals two distinct crystallographic sites, consistent with the results from X-ray diffraction. The projection in the F_1 dimension shows a high-resolution ^{23}Na NMR spectrum with two separate isotropic resonances because the broadening due to second-order quadrupolar interaction has been averaged. Each isotropic peak in the F_1 dimension is related to a subspectrum along the F_2 dimension, from which information about the isotropic chemical shift (δ_{iso}), quadrupole coupling constant ($C_Q = e^2qQ/h$), and asymmetry parameter (η_Q) can be estimated. However, it should be emphasized that because F_2 subspectra often exhibit lineshape distortion and do not contain quantitative information about peak intensities, they were used only as a starting point and restraints in the simulation of 1-D MAS NMR spectra. Final NMR parameter extraction was achieved by comparing spectral features in experimental and simulated 1-D MAS NMR spectra (parts a and b of Figure 6, respectively). Such a combined analysis of the 2-D MQMAS and 1-D MAS NMR spectra yielded the following parameters for slices A and B (with an intensity ratio of 2:1): $\delta_{iso}(A) = 12.5 \pm 0.2$ ppm, $C_Q(A) = 3.0 \pm 0.1$ MHz, $\eta_Q(A) = 0.55 \pm 0.01$; $\delta_{iso}(B) = 9.0 \pm 0.2$ ppm, $C_Q(B) = 3.7 \pm 0.1$ MHz, $\eta_Q(B) = 0.68 \pm 0.01$. We found that the experimental spectrum could not be fitted with an A/B intensity ratio of 1:2. Given that the site occupancy of Na(1)/Na(2) is 1:2, as determined from single-crystal X-ray analysis, spectral assignment can be readily achieved on the basis of their relative intensities. Consequently, resonance A in the ^{23}Na MQMAS spectrum (Figure 7) is therefore assigned to Na(2) and resonance B to Na(1).

In conclusion, we have reported the molten-salt synthesis and structural characterization by single-crystal X-ray diffraction and solid-state NMR spectroscopy of a salt-inclusion stannosilicate. It adopts a new structure and is the first metal silicate that contains both Na^+ and F^- ions in the structural channels. The ^{19}F and ^{29}Si MAS NMR and ^{23}Na MQMAS NMR spectra are consistent with the crystallographic results. This work makes an important addition to the structural chemistry of metal silicates and suggests that the salt-inclusion method is a promising approach for the synthesis of new silicate structures.

Acknowledgment. We thank the National Science Council for support and F.-L. Liao and Prof. S.-L. Wang at National Tsing Hua University for X-ray data collection.

Supporting Information Available: Crystallographic data for **1** in CIF format and X-ray powder patterns. This material is available free of charge via the Internet at http://pubs.acs.org.

IC0514086

(25) MacKenzie, K. J. D.; Smith, M. E. *Multinuclear Solid-State NMR of Inorganic Materials*; Pergamon: New York, 2002.